Changes in physico-chemical properties and water status of durum wheat constituents in pasta due to processing and cooking

Marie Laurent, Reine Barbar, Clémentine Beaudoux, Emma Soubirou, Leslie Lhomond, Adrien Réau, Bernard Cuq

Journal of Cereal Science 112 (2023) 103707

Contents lists available at ScienceDirect

Journal of Cereal Science

journal homepage: www.elsevier.com/locate/jcs

Changes in physico-chemical properties and water status of durum wheat constituents in pasta due to processing and cooking

Marie Laurent [a], Reine Barbar [b], Clémentine Beaudoux [a], Emma Soubirou [a], Leslie Lhomond [a], Adrien Reau [a], Bernard Cuq [b,*]

[a] INRAE, UMR IATE (Université de Montpellier; INRAE; L'Institut Agro Montpellier), Montpellier, France
[b] L'Institut Agro Montpellier, UMR IATE (Université de Montpellier; INRAE; L'Institut Agro Montpellier), Montpellier, France

ARTICLE INFO

Keywords:
Pasta
Durum wheat
Processing
Water interaction

ABSTRACT

Pasta is simply made from durum wheat semolina and water, through a succession of unitary operations. The changes of the interactions between durum wheat constituents and water molecules under different water content conditions provide information on the mechanisms involving wheat constituents and induced by the successive unitary operations. The objective of the present work is to describe the interactions between durum wheat constituents and water molecules in durum wheat semolina, dry pasta, and cooked pasta under different water content conditions using complementary analytical methods at different observation scales. Selected products were investigated by measurements of gelatinization endotherms by DSC, viscosity curves of a suspension by RVA, proton mobility by NMR, and molecular interactions by ATR-FTIR spectroscopy. The measured values describing the interactions between wheat constituents and water molecules are sensitive to changes induced by the process. These results contribute to a better understanding of the modifications induced by the succession of unitary operations on durum wheat constituents, from native semolina to cooked pasta.

1. Introduction

Pasta is an everyday food made from durum wheat semolina and water, through a succession of unitary operations. Semolina and water are mixed, kneaded and structured by extrusion to generate a continuous dough, which is shaped in pasta and then dried. Dry pasta undergo cooking in boiling water at consumers before eating. Thermomechanical treatments during pasta processing induce several mechanisms involving wheat constituents (especially proteins and starch) and water molecules. Cooked pasta qualities depend on the native characteristics of wheat constituents and their processing-induced changes. Several publications explored the changes in wheat constituents during pasta processing (Wagner et al., 2011; Sicignano et al., 2014; Martin et al., 2019). Given the complexity of wheat constituents, complementary analytical methods are required to assess the mechanisms at different scales (molecular, macromolecular, microscopic, and macroscopic) (Bonomi et al., 2012; Diantom et al., 2019). Analyzing the interactions between water molecules and wheat constituents provides relevant information to describe mechanisms involved during pasta processing.

Interactions between water and wheat constituents in suspension in excess water can be described using indirect methods. The measurement of pasting properties during heating has been done using a Rapid Visco Analyzer or a Viscoamylograph. These methods describe the ability of wheat constituents, suspended and partially solubilized in excess water, to generate viscosity during a heating, hot holding and cooling cycle. In dry pasta, viscosity values are sensitive to the crystallinity state of starch granules and to the solubility properties of the protein network (Güler et al., 2002; Bruneel et al., 2010; Tagliasco et al., 2021). There are no data describing the changes in RVA properties induced by the durum wheat pasta manufacturing process.

Interactions between water and wheat constituents in excess water can be described by measuring heating-induced endothermic phenomena, using differential scanning calorimetry (DSC) methods. The crystallinity state of starch granules was evaluated by the measurement of starch gelatinization endotherms. DSC methods were used for native semolina and intermediate products during pasta extrusion (Vansteelandt and Delcour, 1998; Masato et al., 2021) and for dry pasta (Güler et al., 2002; Bruneel et al., 2010; Tagliasco et al., 2021). The diversity of DSC protocols makes difficult to consolidate the values among reported works.

* Corresponding author.
E-mail address: bernard.cuq@supagro.fr (B. Cuq).

https://doi.org/10.1016/j.jcs.2023.103707
Received 24 February 2023; Received in revised form 10 May 2023; Accepted 14 May 2023
Available online 3 June 2023

The molecular nature of interactions and their strength between wheat constituents and water molecules can be investigated by Fourier-transform infrared spectroscopy (FTIR) or low field nuclear magnetic resonance spectroscopy (NMR). The NMR method evaluates the molecular mobility of protons from water molecules and constituents, through the measurement of the distribution of transverse relaxation time T_2 of protons. Several works described pasta by NMR. These works have investigated the influence of process in fresh pasta (Carini et al., 2009; 2010), of adding ingredients in cooked pasta (Curti et al., 2015; Diantom et al., 2019), or of storage time in sterilized pasta (Carini et al., 2013; Diantom et al., 2016). The diversity of sample water contents and of NMR protocols between publications makes a global analysis of the published data rather difficult.

Fourier transform infrared (FTIR) spectroscopy provides information that describes the structure, water interactions, and conformational changes of molecules. FTIR spectroscopy is suited to describe the structure and dynamics of water molecules. In FTIR spectrum, three bands are commonly studied and related to water, starch and amide. This method has been used to study the impact of heat treatments on wheat flour (Iuga and Mironeasa, 2021; Ma et al., 2021), and the impact of processing on wheat constituents in cooked pasta (Garcia Valle et al., 2021).

The objectives of the present work are to use complementary analytical methods to describe the changes in interactions between durum wheat constituents and water molecules during pasta processing. Durum wheat semolina, dry pasta and cooked pasta were characterized at similar specific water content, to eliminate the artefact effects of different water contents. The NMR measurements were performed at the water content of cooked pasta as consumed. Gelatinization endotherms by DSC, viscosity curves by RVA, proton mobility by NMR and molecular interactions by ATR-FTIR spectroscopy were analyzed. The results will contribute to a deeper understanding of wheat constituents modifications induced by pasta processing.

2. Materials and methods

2.1. Raw material

Durum wheat semolina was supplied by Panzani (France) and stored at 4 °C before experiment. Semolina water content (15.8 (±0.1) g water/100 g semolina) was determined by weighing after drying for 2h in an oven at 130 °C (AACC method 44–15.02).

2.2. Pasta processing

Pasta was manufactured using a laboratory Mac30 LAB pasta making machine (Italpast, Parma, Italia). The day before the production, a bucket of semolina was taken out from cold-storage room and warmed to ambient temperature. Just before pasta making, semolina water content was measured using a XM50 desiccator weigher (Precisa, Dietikon, Switzerland). A sample of 5.0 kg of semolina was weighed, introduced in the mixer tank, and mixed for 30 s of 53 rpm. The hydration stage was conducted by adding tap water, previously heated to 40 °C in a thermoregulated kettle. Depending on the semolina water content, the amount of added water (about 1200 g) was defined to obtain a final water content of 47.5% (db). The hydrated semolina was mixed for 20 min at 53 rpm at atmospheric pressure. The hydrated semolina was extruded at constant temperature (40 °C) under vacuum (0.2 atm) with a screw rotation speed of 30 rpm, through a vertical die (70 cylindrical holes of 1.24 mm in diameter). The freshly extruded spaghetti were positioned on metal rods and placed in a CS 40/500-10/S dryer (CTS, Trets, France) at 35 °C and 88% relative humidity (RH). The following drying diagram was applied: 60 min to reach 90 °C and 77% RH; 120 min at 90 °C and 77% RH; 120 min to reach 35 °C and 70%HR; 60 min at 35 °C and 70% RH. Dry pasta batches were collected and stored in hermetic plastic bags.

2.3. Pasta cooking

Dry pasta samples were cooked in boiling water according to the French Standard NF ISO 7304.2. A sample of 100 g of dry pasta (cut to a length of 12 cm) was cooked for 9 min in 2L of boiling water without salt. Dry pasta samples were cooked to the optimum cooking time. Cooked pasta samples were stored in hermetic plastic bags, frozen and freeze-dried for 48 h.

2.4. Pasta grinding

Dry pasta and freeze-dried cooked pasta samples were ground before characterization. Pasta samples were cut in short pieces (1 cm length). Pasta samples were first ground using a Laboratory Mill 3303 (Perten, Sweden) and then using a Cyclotec CT 293 (Foss, Danemark) to limit damage of starch granules.

2.5. Characterization

2.5.1. Water content

Water content of samples was determined in triplicate by weighing after drying in an oven for 2 h at 130 °C according to AACC method 44-15.02.

2.5.2. DSC analysis

The crystallinity state of starch granules was analyzed by using a DSC Q200 (TA Instruments, New Castle, DE, USA) calibrated with indium, using an empty pan as reference. The product sample (about 4 mg) was precisely weighed in a T-zero aluminium pan and mixed with distilled water (1/3 w/v). The pan was hermetically sealed and equilibrated at 20 °C overnight before measurements. The sample was scanned from 25 to 90 °C, at 4 °C/min. Three measurements were conducted for each product. Heat flux variations were recorded as a function of temperature. Thermograms were analyzed using Universal Analysis 2000 software (TA Instruments, New Castle, DE, USA). Endotherm peaks associated with gelatinization were characterized by onset (To), peak (Tp), and conclusion (Tc) temperatures, and by the enthalpy (ΔH). The peak area was used to calculate the amount of non-gelatinized starch, taking into account the dry matter mass of the sample introduced in the pan and using native semolina as reference (equation (1)).

$$\text{Gelatinization degree } (\%) = 100\ \frac{\Delta H_{\text{Semolina}} - \Delta H_{\text{Sample}}}{\Delta H_{\text{Semolina}}} \quad (1)$$

where ΔH_{Sample} and $\Delta H_{\text{Semolina}}$ are the gelatinization enthalpy (J/g dry matter) of pasta sample and native semolina, respectively.

2.5.3. Pasting properties

Pasting properties were investigated using a RVA (Newport Scientific, Warriewood, AUS) following the protocol: 10 s at 25 °C and 960 rpm; 120 s at 25 °C and 160 rpm; 300 s at 160 rpm with heating until 95 °C; 180 s at 95 °C; 300 s at 160 °C with cooling until 25 °C; 300 s at 25 °C and 160 rpm. The RVA software determines pasting characteristics: initial viscosity (cP), pasting temperature (°C), peak viscosity (cP), breakdown viscosity (cP) and final viscosity (cP). Measurements were done in triplicate.

2.5.4. Nuclear magnetic resonance (NMR)

NMR analysis were conducted on samples (about 10 g) that were rehydrated by adding water at ambient temperature in a beaker covered with parafilm, to obtain 62 g water/100 g sample (close to the cooked pasta's water content). After 1 h stabilization, samples were introduced in NMR tubes, weighted and equilibrated for 30 min at 20 °C before analysis. NMR measurements were performed using a time-domain Minispec mq20 spectrometer (Bruker, Wissembourg, Germany) operating at a resonance frequency of 20 MHz. Recycling delay was 2 s.

Experiments were conducted using the combined FID-CPMG sequence. The free induction decay sequence (FID) detected the less mobile protons. The Carre-Purcell-Meiboom-Gill sequence (CMPG) with a 90° pulse followed by several 180° pulses detected the most mobile protons. The acquisition of NMR signals was carried out with the Bruker software. Five samples were analyzed for each product. NMR signal intensity was corrected by sample mass. NMR signals were processed using SigmaPlot software (version 13.0). Mathematical modeling (using a model composed of 1 Gaussian and 4 exponentials) was defined using the Levenberg and Larquardt adjustment method. The mathematical treatment allowed the identification of 5 different proton relaxation peaks, characterized by their relaxation time and intensity.

2.5.5. Fourier transform infrared spectroscopy (FTIR)

The FTIR spectra were collected in the 800-4000 cm^{-1} wavenumber range on a Bruker Vertex 70v Fourier Transform spectrometer (Bruker Optik GmbH, Germany) operating with a Globar source, in combination with a KBr beamsplitter and a DigiTect DLaTGS detector with integrated preamplifier. The optical cell was a Golden Gate diamond ATR system. Spectra were recorded with a resolution of 4 cm^{-1}, automatically adding 128 repetitive scans in order to obtain a good signal-to noise ratio and a high reproducibility. Scans were corrected for the air contribution and were preprocessed using OPUS software (version 7.0) by performing a baseline correction, a 9 points smoothing and a vector normalization for taking into account the effective number of absorbers. Experiments were conducted on samples equilibrated at 58% RH in climatic chambers at 25 °C for about 10 days. Spectra regions of interest were the starch region (940–1185 cm^{-1}) and amide I of proteins (1589–1709 cm^{-1}). For each band of interest, second derivatives were calculated when needed. An emphasis was done on the 3700–3000 cm^{-1} region to compare the O–H stretching absorbance band of samples. The spectra of freeze-dried samples were subtracted to the spectra of powder equilibrated at 58% RH ($A_{Sample\ 58\%} - A_{Freeze\text{-}dried\ sample}$) following the direct difference method. The resulting spectra corresponded to interfacial hydration water. The water band was not processed for cooked pasta because the spectrum of freeze-dried sample was too noisy to allow subtraction of spectra.

2.5.6. Statistical processing

The statistical significance of measured values was verified using single factor analysis of variance (ANOVA) and Tukey test on replicated data using StatGraphicsStratus software.

3. Results

3.1. Analysis of gelatinization endotherms

DSC thermograms and their characteristic parameters for native semolina, dry pasta, and cooked pasta are presented in Fig. 1 and Table 1.

3.1.1. Native semolina

The thermogram of semolina has a specific pattern marked by the presence of an endotherm between 50 and 70 °C, associated with gelatinization of native starch in excess water. Similar DSC endotherms have been reported for durum wheat semolina starch (Cunin et al., 1995; Zweifel et al., 2000). During heating of semolina in excess water, gelatinization corresponds to a progressive loss of crystallinity of amylopectin chains in starch granules, due to thermal and water plasticization.

Table 1
DSC, RVA and NMR characteristics for durum wheat semolina, dry pasta, and cooked pasta. Values with different letters in the same line are significantly different ($p < 0.05$).

	Native semolina	Dry pasta	Cooked pasta
DSC parameters			
Onset temperature (°C)	53.8 (±0.3) ^{b}	57.7 (±0.3) ^{a}	56.3 (±0.5) ^{a}
Peak temperature (°C)	60.9 (±0.2) ^{b}	64.4 (±0.2) ^{a}	64.7 (±0.4) ^{a}
Conclusion temperature (°C)	69.3 (±0.1) ^{b}	71.3 (±1.1) ^{a}	–
ΔT (°C)	15.4 (±0.3) ^{a}	14.0 (±0.8) ^{a}	–
Endotherm surface (J/g)	5.75 (±0.21) ^{a}	5.08 (±0.14) ^{b}	0.19 (±0.15) ^{c}
Gelatinization rate (%)	–	12.9 (±3.8) ^{b}	96.3 (±3.1) ^{a}
RVA parameters			
Initial viscosity (cP)	2.3 (±2) ^{b}	–	85.7 (±38.8) ^{a}
Pasting temperature (°C)	66.0 (±3.9) ^{a}	86.8 (±5.0) ^{b}	–
Peak viscosity (cP)	2660 (±87) ^{a}	892 (±102) ^{b}	–
Breakdown (cP)	730 (±42) ^{a}	93 (±9) ^{b}	–
Final viscosity (cP)	5815 (±145) ^{a}	2566 (±198) ^{b}	2398 (±172) ^{b}
NMR relaxation times			
A protons (μs)	19.9 (±0.03) ^{a}	20.3 (±0.04) ^{a}	17.7 (±0.02) ^{b}
B protons (μs)	132 (±4) ^{b}	123 (±4) ^{c}	168 (±4) ^{a}
C protons (ms)	2.67 (±0.07) ^{a}	2.79 (±0.06) ^{a}	2.18 (±0.24) ^{b}
D protons (ms)	13.1 (±0.4) ^{a}	12.0 (±0.2) ^{b}	8.6 (±0.6) ^{c}
E protons (ms)	44.0 (±1.4) ^{b}	63.3 (±1.3) ^{a}	19.3 (±0.9) ^{c}
NMR relaxation amplitudes			
A protons (AU/g)	35.0 (±3.4) ^{a}	35.9 (±0.9) ^{a}	19.2 (±0.6) ^{b}
B protons (AU/g)	7.1 (±0.2) ^{c}	11.2 (±0.3) ^{b}	11.9 (±0.4) ^{a}
C protons (AU/g)	13.1 (±0.6) ^{a}	12.4 (±0.4) ^{ab}	11.4 (±1.5) ^{b}
D protons (AU/g)	24.1 (±1.5) ^{c}	48.2 (±1.4) ^{b}	65.7 (±4.6) ^{a}
E protons (AU/g)	70.2 (±2.5) ^{a}	41.2 (±1.3) ^{b}	72.5 (±6.8) ^{a}

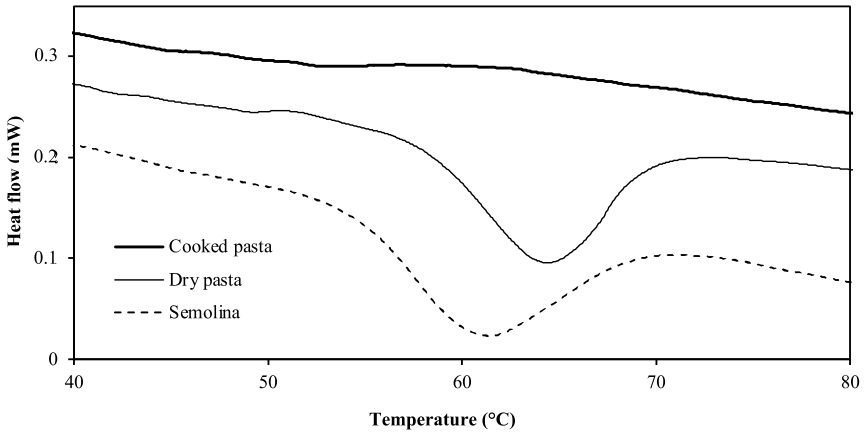

Fig. 1. DSC endotherm curves for native semolina, dry pasta and cooked pasta.

The mechanisms associated with the denaturation of gluten proteins during DSC heating are weakly endothermic compared to starch gelatinization and are neglected. Gelatinization of semolina starch is observed over a temperature range of 53.8–69.3 °C (ΔT = 15.4 °C), with a peak at 60.9 °C and an area of 5.75 J/g. These values are consistent with the large range of published values (Güler et al., 2002; Bruneel et al., 2010; Masato et al., 2021; Tagliasco et al., 2021). The DSC characteristics of durum wheat semolina depend on the proportion of amylose and amylopectin, proportion of A and B starch granules, and mechanical damage of grains (Soh et al., 2006).

3.1.2. Dry pasta

Thermograms of dry pasta display an endotherm between 50 and 79 °C, associated with gelatinization of starch in excess water. Gelatinization of starch in dry pasta is observed over a temperature range of 57.7–71.3 °C (ΔT = 14.0 °C), with a peak at 64.4 °C and an area of 5.08 J/g. Similar DSC endotherms have been reported for starch gelatinization in dry pasta (Cunin et al., 1995; Zweifel et al., 2000; Masato et al., 2021; Tagliasco et al., 2021). Compared to native semolina, DSC gelatinization endotherms are influenced by the extrusion stage and the drying conditions. Several publications have presented DSC values for the intermediate products between native semolina and freshly extruded pasta (Cunin et al., 1995; Vansteelandt and Delcour, 1998; Masato et al., 2021). The hydration, kneading, and extrusion operations do not alter endotherm temperatures but induce a slight decrease in enthalpy, compared to native semolina. Conversely, Zweifel et al. (2000) reported that the temperature of gelatinization endotherms of freshly extruded spaghetti is lower than that of native semolina, reflecting changes in chain arrangement in starch granule during the extrusion. For dry pasta, the measured values of DSC parameters are close, but significantly different from the values determined for native semolina (Table 1). Starch gelatinization is observed over a narrower temperature range, at a higher gelatinization temperature, and with a lower enthalpy, compared to native semolina. During pasta drying, starch undergoes conformational reorganization: crystalline regions of the chains are destabilized by changes in amorphous regions, particularly in the areas of interactions between amylose chains and amylopectin outer branches. The interpretation of DSC endotherms remains difficult because endothermic phenomena are the result of different molecular events, that are often overlapping.

3.1.3. Influence of cooking

DSC analysis of cooked pasta leads to a thermogram marked by the absence of endotherm associated with starch gelatinization. Similar DSC results have been reported for pasta cooked at optimal cooking time or longer (Cunin et al., 1995). For pasta, the surface area of gelatinization endotherms measured by DSC decreases with cooking time. Cooking in boiling water induces an increase in temperature and water content of pasta, necessary to achieve suitable conditions for gelatinization mechanisms to occur. DSC results show that almost all (99%) the starch gelatinization endotherm disappears in cooked pasta. Starch gelatinization and protein insolubilization are the main structural changes observed during cooking. Both transformations involving protein and starch occur at nearly equivalent levels of temperature and moisture content.

3.2. Analysis of pasting properties

RVA viscosity curves and their characteristic parameters for native semolina, dry pasta and cooked pasta are presented in Fig. 2 and Table 1.

3.2.1. Native semolina

The RVA curve of native semolina shows a typical shape, with a very low initial viscosity, a significant increase in viscosity during the heating phase until reaching a viscosity peak, a significant drop in viscosity during the holding phase at 95 °C, and a significant increase in viscosity during cooling and holding at 25 °C. Similar RVA curves for durum wheat semolina have been reported in the literature (Wood, 2009). The semolina is characterized by RVA pasting temperature of 66 °C, which is slightly lower than published data (Bruneel et al., 2010; Tagliasco et al., 2021). The viscosity values (peak, breakdown, and final) measured for native semolina are close to published values (Wood, 2009; Bruneel et al., 2010). Comparison between values remains difficult as they may have been obtained with different protocols.

3.2.2. Dry pasta

The RVA curve of dry pasta shows an overall pattern similar to that of native semolina, but with different viscosity values. The initial viscosity remains almost zero: starch in dry pasta is not able to generate viscosity when cold. During subsequent RVA heating, the viscosity remains low until a temperature of 81 °C, which is significantly lower than that measured for semolina (95 °C). The peak, breakdown, and final viscosities for dry pasta are significantly lower than those measured for native semolina. The extrusion stage induces the formation of a continuous protein network around starch granules, which could impact the RVA viscosity values. The high temperature drying stage induces cross-linking of the protein network around starch granules, which could limit the ability of the starch to generate viscosity during the RVA test. Similar results have been reported in the literature with RVA viscosity values for dry pasta lower than those measured for semolina, for

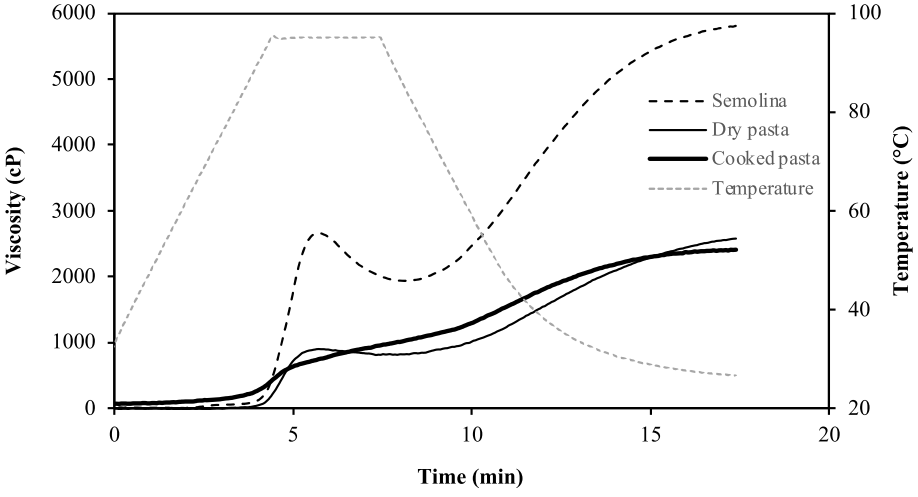

Fig. 2. RVA viscosity curves for native semolina, dry pasta and cooked pasta.

both low or high drying temperatures (Güler et al., 2002; Wood, 2009; Bruneel et al., 2010; Tagliasco et al., 2021). An increase in the temperature of the drying process is found to induce increases in peak, breakdown and final viscosities, due to several possible mechanisms involving amylolytic enzymes, amylose-lipid complexes or annealing effects (Vansteelandt and Delcour, 1998; Güler et al., 2002).

3.2.3. Cooked pasta

The RVA curve of cooked pasta shows a similar pattern to that of dry pasta, but without the drop in viscosity during the holding phase at 95 °C. Cooked pasta are characterized by a high value of initial cold viscosity (86 cP), which reflects the intensity of starch gelatinization mechanisms undergone during cooking. The RVA viscosity curve of cooked pasta is characterized by a progressive increase in viscosity during heating over a large temperature range (between 54 and 88 °C), but without viscosity peak and breakdown. The final viscosity values of cooked pasta are not significantly different from those observed for dry pasta. RVA measurements of cooked pasta describe the contribution of gelatinized starch on the viscosity of the suspension. Pasta cooking in boiling water induces gelatinization of starch granules, which are embedded in a cross-linked protein network. Gelatinization of the starch during pasta cooking results in the exit of amylose chains from the granules, especially from those located on the surface of pasta, which are directly in contact with boiling water during the entire cooking process. Pasta cooking generates heterogeneity in the extent of gelatinization, which could be associated with the large range of temperatures observed during the initial viscosity increase. Starch granule swelling and partial exit of amylose chains during pasta cooking anticipate the effects induced by the RVA heating and holding phases at 95 °C, limiting the viscosity increase and the viscosity drop during the holding phase (Sissons et al., 2012). Similar RVA viscosity profiles have been measured for cooked pasta, with almost no breakdown (Wood et al., 2001).

3.3. Analysis of molecular mobility by NMR

Typical examples of NMR curves measured for native semolina, dry pasta, and cooked pasta are shown in Fig. 3. The position and shape of the relaxation curves differentiate the products. The NMR analyses were performed at similar high water content (163% db), close to water content found in cooked pasta. The observed differences in mobility can be associated with differences in interactions between water molecules and wheat constituents. NMR curves are characterized by a monotonic decay in intensity for relaxation times between 0.01 and 100 ms. Monotonically decreasing NMR relaxation curves have already been reported for fresh pasta with a water content close to 40% db (Carini et al., 2009, 2010, 2013; Curti et al., 2015). The NMR relaxation curve measured for dry pasta is characterized by a shape close to that measured for native semolina, but with slightly higher relaxation intensities whatever the relaxation times. Conversely, the NMR relaxation curve of cooked pasta shows a specific shape, with high intensity values for short relaxation times (<5 ms), a significant drop in intensity for relaxation times close to 5–10 ms, and low intensity values for long relaxation times (>10 ms).

The analysis of NMR curves allows the calculation of characteristic parameters associated with the relaxation of protons with different mobilities. For all products, two FID proton populations (relaxation times close to 20 and 150 μs) and three CPMG proton populations (relaxation times close to 2.5 ms, 10 ms, or 40 ms) are determined. Each proton population is characterized by their relaxation time and relaxation intensity (Table 1). The description of the five proton populations is carried out based on the modeling proposed by Bosmans et al. (2012). The 1st relaxation peak (A protons; 0.02 ms) is associated with hydroxyl groups of rigid crystalline and amorphous structures of starch without contact with water. The 2nd relaxation peak (B protons; 0.08 ms) is associated with protons of mobile amorphous zones in interaction with water. The 3rd relaxation peak (C protons; 0.6 ms) is associated with –CH protons of amorphous zones of starch and protein sheets of gluten, in contact with confined water molecules. The 4th relaxation peak (D protons; 3 ms) corresponds to extra-granular protons with weak interactions with water, to water protons interacting with gluten and with amylose located in the starch extra-granular space. The 5th peak (E protons; 11 ms), corresponds to extra-granular protons with interactions with water. Diantom et al. (2016, 2019) also identified the presence of 5 proton populations with different mobilities in cooked pasta at 130% (db) water content, with relaxation times close to those described in the present study.

3.3.1. Native semolina

For native semolina, five relaxation peaks associated with the protons of populations A, B, C, D, and E are characterized by specific relaxation times and relaxation amplitudes. They describe the native state of organization of wheat constituents in native semolina particles at high water content (163% db).

3.3.2. Dry pasta

There is no data in the literature comparing NMR relaxation spectra of native semolina and the corresponding dry pasta at similar water content. The pasta process induces slight modifications of the

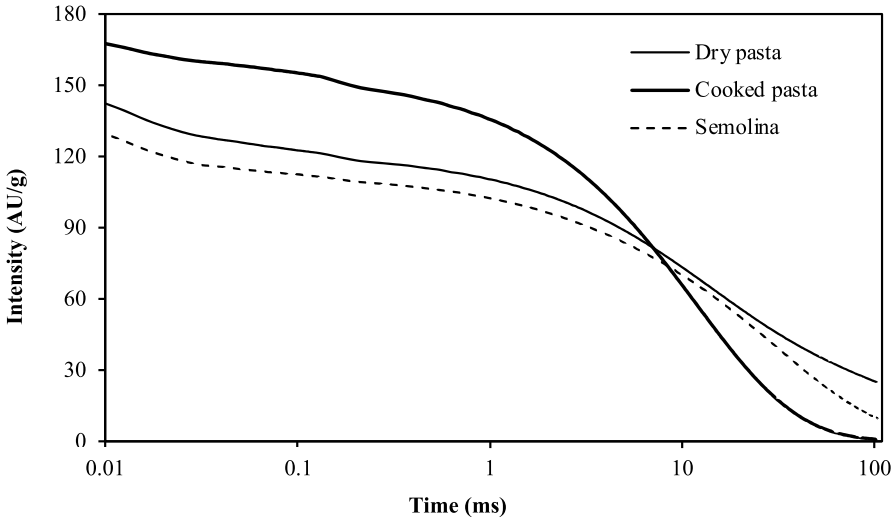

Fig. 3. RMN relaxation curves for native semolina, dry pasta and cooked pasta.

characteristics of NMR relaxation spectra for B, D and E protons, without impacting A and C protons. As expected, pasta process does not modify NMR signals associated with the relaxation of crystalline structures within starch granules (A protons). Compared to native semolina, relaxation times of dry pasta are significantly lower for B and D protons, and higher for E protons. The relaxation amplitudes of dry pasta are significantly higher for B and D protons and lower for E protons. The changes in relaxation behavior of B, D, and E protons could be associated with the structuring mechanisms of gluten proteins, which lead to the formation of a continuous network stabilized by low energy bonds and covalent bridges. These mechanisms involve solubilization and insolubilization reactions of proteins. Some of the changes in B, D, and E protons could also arise from changes involving starch: *(i)* changes in the surface characteristics of starch granules via local shear and/or heating effects during extrusion; *(ii)* from enzymatic reactions at high water activity and shear favoring contacts between enzymes and substrates; *(iii)* effects of hydrothermal conditions on crystal structures during drying at high temperatures. In fresh pasta, Carini et al. (2009) showed that the structuring technology (*i.e.* extrusion, rolling, or vacuum rolling) does not change the interactions of water molecules with wheat constituents as measured by ^{1}H NMR. Conversely, Carini et al. (2010) identified slight impacts of wetting technologies and of structuring technologies (extrusion or rolling) on the NMR relaxation characteristics of A and B protons, associated with changes of the gluten network.

3.3.3. Cooked pasta

The cooking stage of dry pasta induces significant changes in NMR relaxation spectra. Compared to dry pasta, cooked pasta are characterized by significantly lower relaxation times of A, C, D and E protons and relaxation amplitudes of A protons, and also by higher relaxation times of B protons and relaxation amplitudes of B, D, and E protons. The cooking stage induces significant changes in the wheat constituents due to the heat effect in presence of increasing amounts of water. Gelatinization mechanisms result in the loss of crystalline organizations of starch chains in granules and the exit of linear amylose chains out of starch granules located on the surface of pasta. Cooking also results in the deformation of the gluten network (due to the swelling of starch granules) and the ongoing cross-linking mechanisms between protein chains (Wagner et al., 2011). These structures are more accessible to water molecules. The changes in time and amplitude of relaxation of A protons can be associated with gelatinization mechanisms of starch granules and the melting of crystal structures induced by the cooking operation. Diantom et al. (2019) showed that the relaxation intensity of A protons peak is inversely proportional to the degree of gelatinization of pasta ($R^2 = 0.76$) and is related to the melting of amylopectin crystalline zones (Bosmans et al., 2012). Diantom et al. (2016) showed that an increase in the water content of cooked pasta from 130 to 141% (db) results in a decrease in the relaxation time of C, D, and E protons, a decrease in the proportion of D protons, and an increase in the proportion of E protons. Curti et al. (2015) showed for cooked pasta that the relaxation magnitude of E protons is related to the water content ($R^2 = 0.88$). In our results, the differences in relaxation magnitude of E protons at similar water content can be attributed to structural changes of wheat constituents. For cooked pasta at 130% (db) water content, Diantom et al. (2016) showed that the intensity of the relaxation magnitude of A protons increases during storage, with a consequent decrease in relaxation magnitude of B protons, indicating an increase in pasta stiffness, mainly due to the amylopectin retrogradation.

3.4. Analysis by FTIR spectroscopy

The FTIR absorption spectra for native semolina, dry pasta, and cooked pasta are presented in Fig. 4. The characteristic parameters of the FTIR curves associated with the absorption bands of starch and proteins are presented in Table 2. The absorption bands of the 3 products are characterized by several peaks located in the same wavelength ranges, but which differ by their absorption intensities.

Table 2
FTIR characteristics for native semolina, dry pasta and cooked pasta. Values with different letters in the same line are significantly different ($p < 0.05$).

	Native semolina	Dry pasta	Cooked pasta
Characteristic starch FTIR parameters			
Absorbance (x10^3) at 991 cm^{-1}	0.71 (±0.01) ^{b}	0.78 (±0.01) ^{a}	0.58 (±0.01) ^{c}
Absorbance (x10^3) at 1018 cm^{-1}	0.31 (±0.01) ^{b}	0.40 (±0.01) ^{b}	0.49 (±0.01) ^{a}
Absorbance (x 10^3) at 1047 cm^{-1}	0.16 (±0.01) ^{a}	0.17 (±0.01) ^{a}	0.04 (±0.01) ^{b}
Peak absorbance ratio (A_{991}/ A_{1018})	2.29 (±0.03) ^{a}	1.95 (±0.04) ^{b}	1.18 (±0.02) ^{c}
Peak absorbance ratio (A_{1047}/ A_{1018})	0.52 (±0.01) ^{a}	0.43 (±0.04) ^{b}	0.08 (±0.01) ^{c}
Characteristic protein FTIR parameters			
Normalized absorbance (x10^3) at 1628 cm^{-1}	–	0.39 (±0.02) ^{a}	0.29 (±0.06) ^{b}
Normalized absorbance (x10^3) at 1651 cm^{-1}	0.57 (±0.01) ^{a}	0.41 (±0.03) ^{c}	0.47 (±0.06) ^{b}
Normalized absorbance (x10^3) at 1664 cm^{-1}	–	–	0.35 (±0.02)

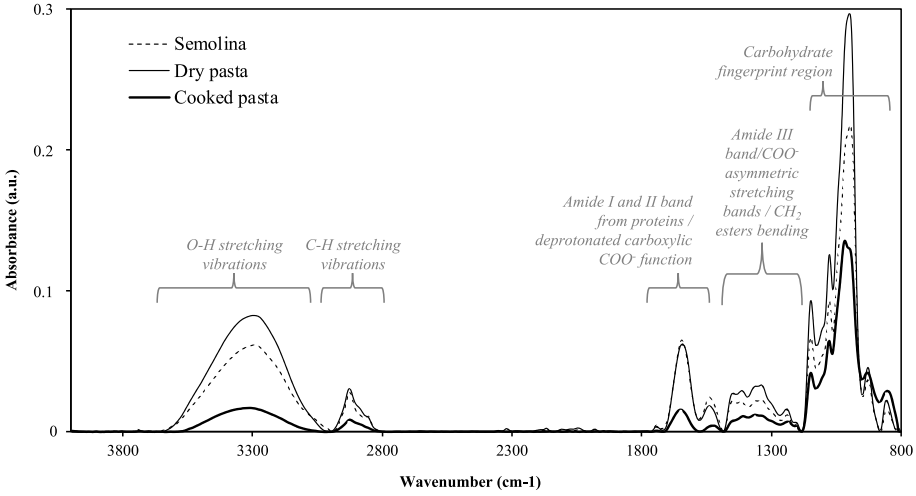

Fig. 4. Raw FTIR absorption spectra for native semolina, dry pasta and cooked pasta.

3.4.1. Native semolina

The second derivative of native semolina starch band has a characteristic shape with the presence of 3 peaks (Table 2). The FTIR region ranging between 1070 and 950 cm^{-1} is a fingerprint of the starch molecular organization (Garcia Valle et al., 2021): absorption at 1047 cm^{-1} is ascribed to ordered structures (e.g. double-helices); absorption at 1022 cm^{-1} is ascribed to amorphous structures; absorption at 1000–995 cm^{-1} is ascribed to hydrated crystalline structures. The second derivative of native semolina amide band shows a peak at 1651 cm^{-1}, corresponding to random structures (Byler and Susi, 1986). The OH stretch band at 3000–3700 cm^{-1} is attributed to different hydrogen bonds formed through OH groups in starch. The broad band with peak at about 3300 cm^{-1} is ascribed to the OH group and reflects the interactions between water molecules and wheat constituents, as well as water-water interactions (free water) via hydrogen bonds (Fig. 4). The water in food products can be classified into free water, freezing bound water, and non-freezing bound water. Free water is not involved in hydrogen bonding with hydrophilic molecules. Freezing-bound water exhibits weak interactions with hydrophilic molecules. Non-freezing bound water forms specific structures with hydrophilic molecules via hydrogen bonds. Vibrations at low-energy levels (*i.e.* low wavenumber) are commonly related to molecules forming strong hydrogen bonds. In contrast, high-energy vibrations (*i.e.* high wavenumber) are ascribed to free water molecules involved only in water-water interactions. The band at 3220 cm^{-1} (Fig. 4) is assigned to water molecules weakly linked by hydrogen bonds to the gluten network (Bock et al., 2013). The band at 3540 cm^{-1} can be assigned to a small number of H-bonds to other water molecules. The band at 3393 cm^{-1} may indicate intermediate water population.

3.4.2. Dry pasta

The FTIR absorption spectra of dry pasta shows a fairly similar pattern to semolina (Fig. 4). Compared to native semolina, the peaks at 991 cm^{-1} and at 1018 cm^{-1} have a significantly higher intensity (Table 2), the peak at 1047 cm^{-1} has a similar intensity and the A_{991}/A_{1018} and A_{1047}/A_{1018} ratios of peak absorbance are lower. The A_{1047}/A_{1018} ratio is commonly considered to quantify the short-range order of starch structures. The A_{991}/A_{1018} ratio reflects the alignment of helices at short order range, which are structures influenced by bonded water molecules (Capron et al., 2007). The A_{991}/A_{1018} ratio showed a sharp decrease in the transition from the wheat flour to the dough, from 1.1 to 0.7, which is in accordance with the decrease observed between semolina and dry pasta. Extrusion had a detrimental effect on the FTIR ratios (Garcia Valle et al., 2021). As for proteins, the amide band of dry pasta shows a rather different pattern from semolina (Fig. 4). The peak at 1651 cm^{-1} has a significantly lower intensity than that of semolina. The amide band of the dry pasta shows an additional peak at 1628 cm^{-1}, which can be ascribed to β-sheets (Byler and Susi, 1986). The semolina processing into dry pasta increased the β-sheets content. The increase of β-sheet content for dry pasta could be expected since this protein structure has been linked to the development of elasticity. The increased formation of β-sheet structures may minimize the water-gluten interactions in the system (with a decrease in 3220 cm^{-1} band as noticed from differential water bands (data not shown), thus reducing the water exposure of the hydrophobic surfaces within the proteins.

3.4.3. Cooked pasta

The FTIR absorption spectra of the starch band of cooked pasta shows a fairly similar pattern to the dry one (Fig. 4), with differences in peaks intensities. Compared to dry pasta, the peak at 991 cm^{-1} and the peak at 1047 cm^{-1} have a significantly lower intensity. The peak at 1018 cm^{-1} has an intensity significantly higher (Table 2) and the A_{991}/A_{1018} and A_{1047}/A_{1018} ratios of cooked pasta are lower. Changes in the A_{1047}/A_{1018} ratio were similar to the A_{991}/A_{1018} ratio during pasta processing and pasta cooking, indicating a strong correlation between hydrated and short-range ordered structures (Garcia Valle et al., 2021). Barbiroli et al. (2013) reported for rice that the pasta-making stages induced changes in starch structure related to the amylopectin fraction. The decrease of the crystalline areas during pasta cooking could suggest amylopectin double helix unraveling and/or amylopectin damage, leading to the formation of short chain linear structures. Cooked pasta presented significant lower A_{991}/A_{1018} ratio which showed the loss of hydrated crystalline structures. Similar trend was reported for heated wheat starch and flour (González et al., 2021). The disruption of short-range ordered structures in starch granules was observed as the A_{1047}/A_{1018} ratio significantly decreased after dough extrusion and cooking. The amide I second derivative of cooked pasta shows a different pattern than the one of dry pasta, with the presence of an additional shoulder at 1664 cm^{-1}. The peak at 1649 cm^{-1} has an intensity significantly higher than the dry pasta peak. The peak at 1628 cm^{-1} has an intensity significantly lower than the dry pasta peak. Coil structures appear at 1664 cm^{-1} emphasizing on conformational restructuring during cooking stage. The larger differences in protein spectra seem to be exhibited for the semolina-dry pasta transition, whereas the dry-cooked pasta transition led only to small changes, especially the appearance of coil structures.

4. Conclusions

The description of the interactions between water molecules and durum wheat constituents by complementary methods (DSC, RVA, NMR, and FTIR) allows to enrich in an original way the comprehension of mechanisms induced by pasta processing and final cooking. The methods complementarity comes from the different observation scales of interactions. Extrusion, drying, and cooking stages induce specific changes in proteins and starch granules, driven by mechanical and hydrothermal stresses, and physicochemical and enzymatic reactions. The study of interactions (at different water contents) between wheat constituents and water molecules gives access to information related to the structuring state of proteins and the destructuring state of starch granules. These methods are complementary to other SE-HPLC approaches to describe protein denaturation and cross-linking reactions. These complementary analytical methods will be adapted to understand the effects of the equipment's type and better control parameters of each of the unitary operations (hydration, kneading, extrusion, drying) during pasta manufacturing process. This approach will also be transposable to study the couscous manufacturing process, also based on durum wheat semolina, and better understand the origin of the end-qualities. It would also be particularly interesting to carry out the interaction analyses under the water content conditions used during the transformation process, *i.e.* at 15% for the native semolina, at 45% for mixing and extrusion, at decreasing water contents (from 45 to 15%) for drying, and at increasing water contents (from 15 to 160%) for cooking.

Declaration of competing interest

The authors declare that they have no known competing financial interests or personal relationships that could have appeared to influence the work reported in this paper

Data availability

No data was used for the research described in the article.

Acknowledgements

This work was supported by BPI France through the PIAVE research program DEFI Blé Dur and by the Occitanie region through the funding Allocations doctorales 2020.

References

Barbiroli, A., Bonomi, F., Casiraghi, M.C., Iametti, S., Pagani, M.A., Marti, A., 2013. Process conditions affect starch structure and its interactions with proteins in rice pasta. Carbohydr. Polym. 92 (2), 1865–1872.

Bock, J.E., Connelly, R.K., Damodaran, S., 2013. Impact of bran addition on water properties and gluten secondary structure in wheat flour doughs studied by attenuated total reflectance Fourier transform infrared spectroscopy. Cereal Chem. 90, 377–386.

Bonomi, F., D'Egidio, M.G., Iametti, S., Marengo, M., Marti, A., Pagani, M.A., Ragg, E.M., 2012. Structure–quality relationship in commercial pasta: a molecular glimpse. Food Chem. 135, 348–355.

Bosmans, G.M., Lagrain, B., Deleu, L.J., Fierens, E., Hills, B.P., Delcour, J.A., 2012. Assignments of proton populations in dough and bread using NMR relaxometry of starch, gluten, and flour model systems. J. Agric. Food Chem. 60 (21), 5461–5470.

Bruneel, C., Pareyt, B., Brijs, K., Delcour, J.A., 2010. The impact of the protein network on the pasting and cooking properties of dry pasta products. Food Chem. 120, 371–378.

Byler, D.M., Susi, H., 1986. Examination of the secondary structure of proteins by deconvolved FTIR spectra. Biopolymers 25 (3), 469–487.

Capron, I., Robert, P., Colonna, P., Brogly, M., Planchot, V., 2007. Starch in rubbery and glassy states by FTIR spectroscopy. Carbohydr. Polym. 68 (2), 249–259.

Carini, E., Curti, E., Littardi, P., Luzzini, M., Vittadini, E., 2013. Water dynamics of ready to eat shelf stable pasta meals during storage. Innov. Food Sci. Emerg. Techno. 17, 163–168.

Carini, E., Vittadini, E., Curti, E., Antoniazzi, F., 2009. Effects of different shaping modes on physicochemical properties and water status of fresh pasta. J. Food Eng. 93, 400–406.

Carini, E., Vittadini, E., Curti, E., Antoniazzi, F., Viazzani, P., 2010. Effect of different mixers on physicochemical properties and water status of extruded and laminated fresh pasta. Food Chem. 122, 462–469.

Cunin, C., Handschin, S., Walther, P., Escher, F., 1995. Structural changes of starch during cooking of durum wheat pasta. LWT - Food Sci. Technol. 28 (3), 323–328.

Curti, E., Carini, E., Diantom, A., Cassotta, F., Najm, N.E.O., D'Alessandro, A., Vittadini, E., 2015. Effect of glycerol and gluten on mechanical properties and 1H NMR mobility of cooked pasta. Food Biophys. 10, 474–480.

Diantom, A., Carini, E., Curti, E., Cassotta, F., D'Alessandro, A., Vittadini, E., 2016. Effect of water and gluten on physico-chemical properties and stability of ready to eat shelf-stable pasta. Food Chem. 195, 91–96.

Diantom, A., Curti, E., Carini, E., Boukid, F., Mattarozzi, M., Vodovotz, Y., Careri, M., Vittadini, E., 2019. A multi-scale approach for pasta quality features assessment. LWT - Food Sci. Technol. 101, 285–292.

Garcia-Valle, D.E., Bello-Pérez, L.A., Agama-Acevedo, E., Alvarez-Ramirez, J., 2021. Effects of mixing, sheeting, and cooking on the starch, protein, and water structures of durum wheat semolina and chickpea flour pasta. Food Chem. 360, 129993.

González, M., Vernon-Carter, E.J., Alvarez-Ramirez, J., Carrera-Tarela, Y., 2021. Effects of dry heat treatment temperature on the structure of wheat flour and starch in vitro digestibility of bread. Int. J. Biol. Macromol. 166, 1439–1447.

Güler, S., Köksel, H., Ng, P.K.W., 2002. Effects of industrial pasta drying temperatures on starch properties and pasta quality. Food Res. Int. 35 (5), 421–427.

Iuga, M., Mironeasa, S., 2021. Simultaneous optimization of wheat heat moisture treatment and grape peels addition for pasta making. LWT - Food Sci. Technol. 150, 112011.

Ma, Y., Zhang, H., Xu, D., Jin, Y., Xu, X., 2021. Wheat flour superheated steam treatment induced changes in molecular rearrangement and polymerization behavior of gluten. Food Hydrocoll 118, 106769.

Martin, C., Morel, M.H., Reau, A., Cuq, B., 2019. Kinetics of gluten protein-insolubilisation during pasta processing: decoupling between time- and temperature-dependent effects. J. Cereal. Sci. 88, 103–109.

Masato, O., Kentaro, M., Tatsuro, M., Akio, F., Yukako, H., Yasuki, M., 2021. Effects of drying temperature on the properties of starch in pasta. LWT - Food Sci. Technol. 145, 111171.

Sicignano, A., Di Monaco, R., Masi, P., Cavella, S., 2014. From raw material to dish: pasta quality step by step. J. Sci. Food Agric. 95, 2579–2587.

Sissons, M., Marchylo, R., Abecassis, J., Cubbada, R.J.E., D'Egidio, M.G., 2012. In: Sissons, M.J., Abecassis, J., Marchylo, B., Carcea, M. (Eds.), Methods Used to Assess and Predict Quality of Durum Wheat, Semolina, and Pasta, Durum Wheat: Chemistry and Technology. AACC International Press, pp. 213–234.

Soh, H.N., Sissons, M.J., Turner, M.A., 2006. Effect of starch granule size distribution and elevated amylose content on durum dough rheology and spaghetti cooking quality. Cereal Chem. 83 (5), 513–519.

Tagliasco, M., Fogliano, V., Pellegrini, N., 2021. Pasta regrind: the effect of drying temperature on its functionality as a novel ingredient. Food Struct. 30, 100230.

Vansteelandt, J., Delcour, J.A., 1998. Physical behavior of durum wheat starch (*triticum durum*) during industrial pasta processing. J. Agric. Food Chem. 46, 2499–2503.

Wagner, M., Morel, M.A., Bonicel, J., Cuq, B., 2011. Mechanisms of heat-mediated aggregation of wheat gluten protein upon pasta processing. J. Agric. Food Chem. 59 (7), 3146–3154.

Wood, J.A., Batey, I.L., Hare, R.A., Sissons, M.J., 2001. A comparison of Australian and imported spaghetti. Food Austr. 53, 349–354.

Wood, J.A., 2009. Texture, processing and organoleptic properties of chickpea-fortified spaghetti with insights to the underlying mechanisms of traditional durum pasta quality. J. Cereal. Sci. 49, 128–133.

Zweifel, C., Conde-Petit, B., Escher, F., 2000. Thermal modifications of starch during high-temperature drying of pasta. Cereal Chem. 77 (5), 645–651.